Dynamics of Bipedal Gait Part II: Stability Analysis of a Planar Five-Link Biped

Yildirim Hurmuzlu

Mechanical Engineering Department
Southern Methodist University
Dallas,TX 75275

February 24, 1998

Abstract

A general approach based on discrete mapping techniques is presented to study stability of bipedal locomotion. The approach overcomes difficulties encountered by others on the treatment of discontinuities and nonlinearities associated with bipedal gait. A five-element bipedal locomotion model with proper parametric formulation is considered to demonstrate the utility of the proposed approach. Changes in the stability of the biped as a result of bifurcations in the four-dimensional parameter space are investigated. The structural stability analysis uncovered stable gait patterns that conform to the prescribed motion. Stable non-symmetric locomotion with multiple periodicity was also observed, a phenomenon that has never been considered before. Graphical representation of the bifurcations are presented for direct correlation of the parameter space with the resulting walking patterns.

The bipedal model includes some idealizations such as neglecting the dynamics of the feet and assuming rigid bodies. Some additional simplifications were performed in the development of the controller that regulates the motion of the biped.

1 Introduction

Analysis of dynamics and stability of bipedal gait and development of control algorithms to regulate the motion of bipedal automata is a challenging problem which has prompted ongoing research efforts by many investigators.

Furusho and Matsubuchi (1986) considered a five-element biped. The equations of motion were linearized about the upright position of the biped and proportional plus derivative feedback are used at the individual joints. The system behavior was analyzed on a two dimensional subspace of the phase space that represents the dominant poles of the linear system. The stability was tested by establishing a recursive relation among successive velocities at foot contact. Although this method was never characterized in the article as discrete mapping, it was the first attempt in studying the stability of bipedal gait by some type of a discrete map. But, the system was simplified to an extent that the resulting dynamics represented a very restricted subset of the actual behavior.

Katoh and Mori (1984) have considered a simple biped with telescopic legs. The equations of motion were partially linearized about vertical stance, and coupled van der Pol equations were used to prescribe the locomotion. The model has also included the impact of the lower limbs with the walking surface, and the article stressed the unavoidability of the impact problem in bipedal walk. Stability of the walking motion was established by proving convergence to the dynamics prescribed by the van der Pol equations and few numerical examples that demonstrate limit cycles on the phase plane.

Hemami et al. authored several articles studying the upright stability of inverted pendulums using Lyapunov's second method. In Hemami and Chen (1984) a two link inverted pendulum model, complete with ligament and muscle structures was constructed. Stability of the system about operating points was guaranteed by constructing feedback strategies based on Lyapunov functions. Zheng and Hemami (1984) have considered impact effects of the biped with its environment. Disturbances resulting from the velocity jumps as a result of impact were eliminated by using appropriate feedback functions. The general focus of Hemami et al. is feedback stabilization of inverted pendulum models that are correlated mostly with non locomotive actions (jumping, side sway, frontal sway etc.) of man made bipedal systems. Lyapunov's method has been proved to be an effective tool in developing robust controllers to regulate such actions. Its applicability to study the stability of the overall gait still remains to be an open question.

One of the latest work addressing stability of gait has appeared in Vukobratovic et al. (1990). The analysis is based on the concept of *practical*

stability which is introduced by the authors. The definition identifies three regions in the state space. The system is said to be stable if for all state trajectories starting from a subspace X^I reach a subspace X^F within a time interval τ_s while remaining in a subspace X^t. As implied by the term *practical*, this is not a formal definition that conforms to the general notion of stability as it understood in the area of nonlinear dynamics. In general, one can identify invariant solutions where the state is trapped in a periodic orbit but deviates from it when perturbed along the unstable manifold. Yet, according to the pactical stability definition these solutions should be identified as stable. Based on the definition of *practical stability* a two stage control methodology is developed. In the first stage, the control algorithm guarantees the realization of the nominal motion in the absence of disturbances. Then a decentralized control scheme is built assuming no dynamic coupling between the joints and is incorporated into the existing controller. Finally additional control loops are applied to take into account the nonlinear coupling effects among various joints. The control strategy is applied to a nine d.o.f. bipedal model, and numerical simulation is performed to demonstrate the effectiveness of the proposed schemes. The approach is novel since the equations of motion are kept in nonlinear forms, actuator models are included and a complicated example is worked out. Yet, the question arises whether such sophistication in control strategy is needed at all? Furthermore, the stability analysis is convoluted with the proposed control scheme, the method serves as a development tool rather than testing tool that can be used to study the stability of bipedal systems in general.

Bipedal locomotion systems are highly nonlinear, thus a thorough stability analysis necessitates the inclusion of nonlinear effects. Such analysis should bring a formal definition to the stability of gait and provide mechanisms that can be used to capture the complicated facets of the nonlinear behavior. Stability analyses based on Lyapunov's second method are ad-hoc, primarily because of the difficulties associated with constructing Lyapunov functions that are applicable to a general class of systems.

In the present article we adopt a different approach to the study and control of bipedal systems. First, we introduce a methodology to define and analyze the stability of bipedal locomotion in general. Then, we will synthesize a five element, bipedal system based on the objective functions of Part I. The system includes a controller that tracks desired trajectories during the continuous phases of the step cycle (between successive ground contacts). Finally, we perform a parametric analysis, to correlate the four-dimensional parameter space with the stability and dynamics of the overall gait. Graphical representation of a subset of possible motions in the four

dimensional parameter space are presented to evaluate the preformance of the controller and determine its limitations.

2 Stability analysis

In this article, the approach to the stability analysis takes into account two generally excepted facts about bipedal locomotion. The motion is discontinuous because of the impact of the limbs with the walking surface, Hurmuzlu and Moskowitz (1986), Katoh and Mori (1984) and Zheng (1989). The dynamics is highly nonlinear and linearization about vertical stance should be avoided, Hurmuzlu and Moskowitz (1987) and Vukobratovic (1990).

Given the two facts that have been presented above we propose to apply discrete mapping techniques to study the stability of bipedal locomotion. This approach has been applied previously to study of the dynamics of bouncing ball (Guckenheimer and Holmes, 1985) and to the study of vibration dampers (Holmes and Shaw, 1983 and Shaw and Shaw, 1989). The approach eliminates the discontinuity problems, allows the application of the analytical tools developed to study nonlinear dynamical systems, and brings a formal definition to the stability of bipedal locomotion.

The method is based on the construction of a first return map by considering the intersection of periodic orbits with an n-1 dimensional cross section in the n dimensional state space. There is one complication that will arise in the application of this method to bipedal locomotion. Namely, different set of kinematic constraints govern the dynamics of various modes of motion. Removal and addition of constraints in locomotion systems has been studied before by Hemami and Wyman (1979). They describe the problem as a two point boundary value problem where such changes may lead to changes in the dimensions of the state space required to describe the dynamics. Due to the basic nature of discrete maps, the events that occur outside the cross section are ignored. The situation can be resolved by taking two alterative actions. In the first case a mapping can be constructed in the highest dimensional state space that represents all possible motions of the biped. When the biped exhibits a mode of motion which occurs in a lower dimensional subspace, extra dimensions will be automatically included in the invariant subspace. Yet, his approach will complicate the analysis and it may not be always possible to characterize the exact nature of the motion. An alternate approach will be to construct several maps that represent different types motion, and attach various conditions that reflect the particular type of motion. We will adopt the second approach in this article. Accordingly, for no slip walking, without

the double support phase, a mapping $\mathbf{P}_{nsls}$ is obtained as a relation between the state $\mathbf{x}$ immediately after the contact event of a locomotion step and a similar state ensuing the next contact. This map describes the behavior of the intersections of phase trajectories with a Poincaré section Σ_{nsls} that can be defined as

$$\Sigma_{nsls} = \{(\mathbf{x}, \dot{\mathbf{x}}) \in \Re^n \mid x_T(\mathbf{x}) > 0, y_T(\mathbf{x}) = 0 \mid \dot{y}_T^+(\mathbf{x}) > 0, \left|\frac{\hat{F}_{rx}}{\hat{F}_{ry}}\right| < \mu, \left|\frac{F_{rx}}{F_{ry}}\right| < \mu, F_{ry} > 0\}, \quad (1)$$

where x_T and y_T are the x and y coordinates of the tip of the swing limb respectively. The first two conditions in Eq.(1) establish the Poincaré section (the cross section is taken immediately after foot contact during forward walking). Whereas, the attached four conditions denote no double support phase, no slip impact, no slippage of pivot during the single support phase and no detachment of pivot during the single support phase respectively. For example, to construct a map representing no slip running, the last condition will be removed to allow pivot detachments as they normally occur during running. We will not elaborate on all possible maps that may exist for bipedal locomotion, but we note that the approach can address a variety of possible motions by construction of maps with the appropriate set of attached conditions.

The discrete map obtained by the procedure described above can be written in the following general form

$$\xi_i = \mathbf{P}(\xi_{i-1}) \quad (2)$$

where ξ is the n-1 dimensional state vector, and the subscripts denote the i^{th} and $i-1^{st}$ return values respectively.

Periodic motions of the biped correspond to the fixed points of $\mathbf{P}$ where

$$\xi^* = \mathbf{P}^k(\xi^*). \quad (3)$$

where $\mathbf{P}^k$ is the k$^{\text{th}}$ iterate. Stability of $\mathbf{P}^k$ reflects the stability of the corresponding flow. The fixed point ξ^* is said to be stable when the eigenvalues ν_i, of the linearized map,

$$\delta\xi_i = \mathbf{D}\mathbf{P}^k(\xi^*)\ \delta\xi_{i-1} \quad (4)$$

have moduli less that one.

This method has several advantages. First, the stability of gait now agrees with the formal stability definition accepted in nonlinear mechanics. Eigenvalues of the linearized map (Floquet Multipliers) provide quantitative measures of the stability of bipedal gait. Finally, to apply the analysis to locomotion one only requires the kinematic data that represent all the relevant degrees of freedom. No specific knowledge of the internal structure of the system is needed.

In general, the exact form of $\mathbf{P}$ cannot be obtained in closed form. For example, if the system under investigation is a numerical model of a man made machine, the equations of motion will be solved numerically to compute the fixed points of the map from kinematic data. Then stability of each fixed point will be investigated by computing the Jacobian using numerical techniques. This procedure will be demonstrated for the five-element bipedal model in the ensuing sections. Whereas, if the system in consideration is an experimental prototype, kinematic data will be obtained by measurement and various types of perturbations will be used to investigate the stability. The method can also be applied to the human system. Yet, the complexity of the human locomotor brings about many challenging questions. The number measurements required to capture the dynamic behavior, the external perturbation methods that have to be employed to measure stability are important open questions that are beyond the scope of the present article.

3 Application to the Five-Element Bipedal System

During its motion the biped is subject to repeated disturbances caused by the contact of the lower limbs with the ground surface. Perturbations resulting from the contact event are not directly controllable because the actuators cannot generate impulsive moments to compensate for the effect of contact forces that arise during impact. All the previous work addressing the control of gait are based on some type of trajectory tracking during the continuous phases of locomotion. In some cases, the effect of impulsive forces are neglected altogether to avoid the complications that may arise due to repeated disturbances. In others, specific results are presented that correspond to a very limited choice of parameter values where superior convergence rates can be readily achieved. Yet, the question of the effect of increasing tracking errors on the overall locomotion picture is a rarely addressed issue. Does the motion looses its stability altogether, or some other type of anomalous gait may emerge during which stability is still conserved? For example, the loco-

motion of an amputee may be stable, yet it may not conform to any accepted notion of normal locomotion. Study of anomalous motions is important, and may lead to better understanding of human gait abnormalities. One may create simplified biped models and attempt to induce specific types of abnormalities to better understand the dynamics of the more realistic cases. This study does not address the human gait in any sense. But, it demonstrates the complexity of the motion of a system which is substantially simpler than the human being.

The control strategy in the present work is based on trajectory tracking during the forward swing motion only. The controller proposed below is a computed torque algorithm that is based on full state feedback and assumes perfect knowledge of the system parameters. Controllers of this form are practically limited because of the latter requirement. Yet, the subsequent analysis demonstrates the dynamic behavior for a "best scenario controller". With this added advantage, we will demonstrate below that the biped exhibits very complicated dynamic behavior. The system may generate stable gait patterns that are entirely different than the ones prescribed by the objective functions.

3.1 Control law

Equations of motion of the biped during the forward swing phase can be written as:

$$\dot{\mathbf{x}} = \mathbf{f}(\mathbf{x}) + \mathbf{b}(\mathbf{x})\mathbf{u} \tag{5}$$

Here $\mathbf{x} = \{x_1, \ldots, x_{10}\}^T$, is the 10-dimensional state vector, $\mathbf{u} = \{u_1, \ldots, u_5\}^T$ is the 5-dimensional control, $\mathbf{f}$ and $\mathbf{b}$ are vector fields. Also, the dot indicates differentiation with respect to time. The constraint relations that we seek to prescribe during the motion can be written as,

$$\mathbf{S}_\omega(\mathbf{x}) = 0, \omega \in \Re^4 \tag{6}$$

where $\mathbf{S}_\omega = \{S_1, \ldots, S_5\}^T$ is the constraint function and depends on $\omega = \{V_p, H_m, S_L, \sigma\}$, the vector of locomotion parameters as described in Part I. We drop ω from our notation for simplicity and let,

$$\dddot{\mathbf{S}} := \mathbf{C}_1\ddot{\mathbf{S}} + \mathbf{C}_2\dot{\mathbf{S}} + \mathbf{C}_3 = 0 \tag{7}$$

where $\mathbf{C}_1$, $\mathbf{C}_2$ and $\mathbf{C}_3$ are 5 x 5 matrices containing the design parameters that will be explained below. If S_i is a holonomic constraint (ex. S_1), then i^{th} row of $\mathbf{C}_1$ is set to $\mathbf{e}_i$, whereas if the constraint is non-holonomic (ex.

S_2), then the i$^{\text{th}}$ row of $\mathbf{C}_1$ is set to $\mathbf{0}$ and the i$^{\text{th}}$ row of $\mathbf{C}_2$ is set to $\mathbf{e}_i$ where $\mathbf{e}_1 = \{1, 0, \ldots, 0\}$, $\mathbf{e}_2 = \{0, 1, \ldots, 0\}$, etc. The matrices $\mathbf{C}_2$ and $\mathbf{C}_3$ are diagonal and contain parameters that can be chosen such that the solution set of $\tilde{\mathbf{S}}$ is asymptotically stable about the origin (i.e. $S_i \rightarrow 0$ as t$\rightarrow$0).

We use Eqs. (10), (11), (16), (17) and (19) of Part I to write $\tilde{\mathbf{S}}$ in the form

$$\tilde{\mathbf{S}} = \mathbf{G}(\mathbf{x})\dot{\mathbf{x}} + \mathbf{H}(\mathbf{x}) \tag{8}$$

where $\mathbf{G}$ and $\mathbf{H}$ are 5x5 vector valued functions. Using Eq. (5) to eliminate $\dot{\mathbf{x}}$ from Eq. (8), solving for the control vector $\tilde{\mathbf{u}}$ and dropping $\mathbf{x}$ to simplify the notation yields

$$\tilde{\mathbf{u}} = -(\mathbf{G}\mathbf{b})^{-1}(\mathbf{G}\mathbf{f} + \mathbf{H}) \tag{9}$$

Equation (9) represents a nonlinear feedback law which expresses the controls in terms of the ten state variables.

3.2 Symbolic derivation of $\mathbf{P}_{nsls}$

The control algorithm presented above allows us to prescribe a hierarchical approach to the constraint space by appropriate selection of the approach parameters in the matrices $\mathbf{C}_2$ and $\mathbf{C}_3$ of Eq. (7). However, in the present study we adopt a uniform approach and choose the matrices $\mathbf{C}_1$, $\mathbf{C}_2$ and $\mathbf{C}_3$ as follows

$$\mathbf{C}_1 = diag\{1, 0, 1, 1, 1\} \tag{10}$$

$$\mathbf{C}_2 = diag\{\alpha, 1, \alpha, \alpha, \alpha\} \tag{11}$$

$$\mathbf{C}_3 = diag\{\beta, \lambda_1, \beta, \beta, \beta\} \tag{12}$$

where,

$$\lambda_{1,2} = -\frac{\alpha}{2} \pm \sqrt{\frac{\beta^2}{4} - \alpha\beta} \text{ and } \beta > 4\alpha > 0 \tag{13}$$

Now Equation (7) can be solved for $\mathbf{S}$.

First we obtain the expressions of the angular displacements and velocities at $t > t_0$ in terms of the locomotion parameters, initial time t_0 and initial values of the angular displacements and velocities . We use Eqs. (11), (12), (17), (18) and (20) of Part I and their time derivatives to obtain

$$\phi_2(t) = \sigma + S_4(t) \tag{14}$$

$$\phi_1(t) = -\frac{\phi_2(t)}{2} + \arcsin\left[\frac{\int_{t_0}^{t} S_2(t)\, dt + \eta_1(t)}{\cos\frac{\phi_2(t)}{2}}\right] \tag{15}$$

$$\phi_3(t) = S_1(t) - \phi_1(t) - \phi_2(t) \tag{16}$$

$$\phi_5(t) = \begin{cases} 2\arccos\sqrt{\frac{\eta_2^2(t)+\eta_3^2(t)}{4}} & \text{for} \quad \phi_5(t_0) > 0 \\ -2\arccos\sqrt{\frac{\eta_2^2(t)+\eta_3^2(t)}{4}} & \text{for} \quad \phi_5(t_0) < 0 \end{cases} \tag{17}$$

$$\phi_4(t) = S_1(t) - \frac{\phi_5(t)}{2} - \arctan\left[\frac{\eta_2(t)}{\eta_3(t)}\right] \tag{18}$$

where

$$\begin{aligned} \eta_1(t) &= -V_p(t-t_0) \\ &\quad - \frac{\sin S_1(t) - \sin S_1(t_0) - \sin\phi_1(t_0) - \sin\left[\phi_1(t_0)+\phi_2(t_0)\right]}{2} \end{aligned} \tag{19}$$

$$\eta_2(t) = 2S_5(t) - \sin\phi_1(t) - \sin\left[\phi_1(t)+\phi_2(t)\right] - 2\sin S_1(t) \tag{20}$$

$$\begin{aligned} \eta_3(t) &= 2S_3(t) + 8\frac{H_m}{S_L^2} + H_m \\ &\quad + \left\{S_5(t) - \sin\phi_1(t) - \sin\left[\phi_1(t)-\phi_2(t)\right] - \sin S_1(t)\right\}^2 \end{aligned} \tag{21}$$

$$\dot{\phi}_1(t) = -\frac{S_1(t) + V_p + \dot{S}_1(t)\cos S_1(t) + \dot{S}_4(t)\cos\left[\phi_1(t)+\phi_2(t)\right]}{\cos\phi_1(t) + \cos\left[\phi_1(t)+\phi_2(t)\right]} \tag{22}$$

$$\dot{\phi}_2(t) = \dot{S}_4(t) \tag{23}$$

$$\dot{\phi}_3(t) = \dot{S}_1(t) - \dot{\phi}_2(t) \tag{24}$$

$$\dot{\phi}_4(t) = \frac{-2\gamma_1(t)}{\sin\left[\frac{\phi_5(t)}{2}\right]} \tag{25}$$

$$\dot{\phi}_5(t) = \frac{-2\gamma_2(t)}{\sin\left[\frac{\phi_5(t)}{2}\right]} \tag{26}$$

We simplified the notation by leaving the terms $S_i(t)$, $\dot{S}_i(t)$ and $\int_{t_0}^{t} S_2(t)$ unevaluated in the above equations. We also did not present the expressions for $\gamma_1(t)$ and $\gamma_1(t)$. These expressions are excessively long and the calculations to derive these velocities are relatively straightforward. We used kinematic relations and $\dot{S}_i(t)$, which linearly depend on these velocities to obtain the final expressions.

Equations (25) and (26) reflect singular positions at $\phi_5 = 0, \pm\pi$. These singularities correspond to the fully collapsed and extended swing knee configurations respectively.

The y coordinate of the swing limb can be written as

$$y_T(t) = S_3(t) + \frac{1}{2}\{\cos\phi_1(t) + \cos[\phi_1(t) + \phi_2(t)] - \cos[-S_1(t) + \phi_4(t)] - \cos[-S_1(t) + \phi_4(t) + \phi_5(t)]\} \quad (27)$$

Equation (27) depends on the values of the angular positions at $t = t_0$ and the time t. At contact

$$y_T(t_c) = 0 \quad (28)$$

Equation (28) depends on t_c only, yet the exact solution requires the usage of numerical techniques. Once calculated, t_c can be substituted into Eqs. (14) through (26) to compute the remainder of the unknown quantities. Finally, we substitute the angular positions and velocities at the instant of contact in Eqs. (2) and (3) of Part I to incorporate the impact and switching to obtain the mapping from the initial state to the state immediately after contact.

4 Numerical Simulation and Analysis of $\mathbf{P}_{nsls}$

The overall behavior is governed by the union of two solution sets (equation of motion during the single support phase and the impact and switching equations). We now focus on the interaction of these solution sets and the possible outcomes of this interaction. Numerical analysis is carried out by selecting the control parameters such that $\lambda_1 = -6$ and $\lambda_2 = -7$ to assure higher rates of convergence for trajectory tracking.

4.1 Fixed Points of $\mathbf{P}_{nsls}$

The constrained motion possesses a singular point at $\phi_5 = 0$. This singularity forms a hyperplane which bisects the state space into two disjoint supspaces; the positive subspace where $\phi_5 > 0$ and the negative subspace where $\phi_5 < 0$. Trajectories that start from either subspace do not cross to the other. Solution curves of the prescribed motion $\mathcal{M}_c$ also include two portions $\mathcal{M}_c^+$ and $\mathcal{M}_c^-$ located on either side of hyperplane representing $\phi_5 = 0$. The swing limb is bent forwards during the forward motion when the solution conforms with $\mathcal{M}_c^+$, or it is bent backwards when it conforms with $\mathcal{M}_c^-$. The condition of the swing knee during each step depends on the direction of the knee flexion at the onset of the particular step (ϕ_5^+). When the system encounters the contact, the switching causes the exchange of the stance and swing knee angles. Accordingly, the state of the stance knee at the end of a particular step (ϕ_2^-) also affects the condition of the swing knee during

the ensuing step. Yet, the kinematic constraints fix the stance knee at a bias of σ, which is chosen as a positive constant. Therefore, the motion that conforms to the kinematic constraints corresponds to $\mathcal{M}_c^+$. However, when the motion deviates from the constraints for various reasons, we may expect the trajectories to crisscross from one subspace to the other as a result of switching. As we will see below, a special class of periodic motions which exhibit crisscrossing of state trajectories are indeed observed in certain parameter regimes. Here, solutions ξ^* of Eq. (3) are classified under two general categories:

1. **Type I** Cycles

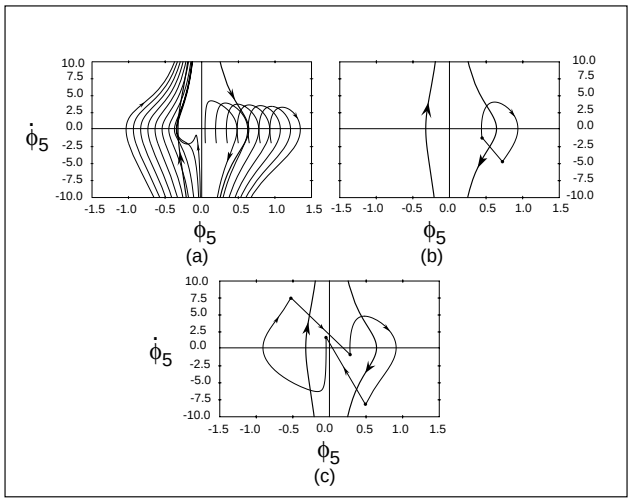

Figure 1: Type I and Type II attractors for $V_p = 1.4$m/s, $H_m = 0.05$m, $S_L = 0.82$m and $\sigma = 0.1$ radians.

TYPE I cycles are periodic solutions that include one contact per cycle. Figure (1.a) represents the cross section of the phase space taken at $\omega = \{1.4, 0.05, 0.82, 0.1\}$. Trajectories that start from an initial ϕ_5 in the the right hand plane where $\phi_5 > 0$, tend to negative infinity as they approach the singularity ($\phi_5 = 0$) along $\mathcal{M}_c^+$. Whereas, trajectories in the left hand plane tend to positive infinity as they approach the singularity along $\mathcal{M}_c^-$. The phase trajectories converge exponentially to $\mathcal{M}_c^+$ and $\mathcal{M}_c^-$ for $t > t_0$. The tendency of state trajectories approaching the singular position is actually a natural consequence of the motion in $\mathcal{M}_c$. We have prescribed a quadratic tip trajectory accompanied by forward motion. In the absence of the walking surface, tip of the swing limb tracks the quadratic trajectory even for negative y_T values. This

action forces the swing knee to extend further so that the tip is kept on the quadratic path, eventually leading to the singular configuration. Figure (1.b) depicts the phase plane picture of the steady state behavior when we incorporate the contact. The configuration depicted in the figure, reveals a closed orbit that includes a portion of a state trajectory accompanied by a sudden transfer. Subsequent calculation of the characteristic multipliers at this limit cycle yields $\max[\mathrm{mod}(\nu_i)] = 0.08$, which denotes a strongly stable attractor. The numerical study for the present system produces **Type I** cycles that are located in the positive subspace. Cycles of this class have not been encountered in the negative subspace.

2. **TYPE II**$^{(n)}$ Cycles

   We define the **TYPE II**$^{(n)}$ cycles as periodic solutions that include n contacts per period. Figure (1.c) depicts the second cycle, which appears when contact is incorporated. This closed orbit is formed by portions of dynamic trajectories that are located in opposite sides of the singular point. During the motion that corresponds to this solution, the biped takes one step during which the swing knee is bent backwards, followed by a step during which the knee is bent forwards.

   The numerical search for this class of cycles produced closed orbits that always include state trajectories that cross over at least once per period. We did not encounter any **TYPE II**$^{(n)}$ that lie entirely in either the positive or the negative subspaces.

4.2 Structural Stability of the Fixed Points of $\mathbf{P}_{nsls}$

The focus of this section is to investigate the structural stability of the limit cycles subject to variations in the components of the parameter vector ω.

Figure (2) depicts bifurcations of **Type I** cycles that take place at $\sigma = 0.1$ radians and $\mathrm{H}_m = 0.05$ m when progression velocity and step length are varied. We obtain the bifurcation diagram by plotting c_1 versus ϕ_5. We use c_1 instead of S_L as one of the variables. This choice stretches the bifurcation diagram for very small step lengths and provides better visualization of the diagrams. Solid lines in the figure represent stable cycles while dashed lines represent unstable cycles. For progression velocities $\mathrm{V}_\mathrm{p} < 1.2$ m/s, loci of stable limit cycles are given by a single branch. This branch ends when it reaches the horizontal axis where $\phi_5^+ = 0$. At this point a very complex set of bifurcations are encountered. We will return to these bifurcations later in

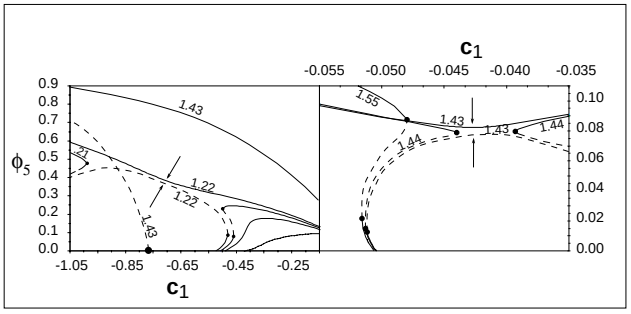

Figure 2: Bifurcation diagrams at $\sigma = 0.1$ radians and $H_m = 0.05$ m.

this section. When the velocity is increased, a codimension two bifurcation occurs and the three limit cycles emerge as this branch folds creating two saddle-node (SN) bifurcations (point D). A third SN bifurcation enters the picture from the left, revealing existence of two more cycles for short step lengths. As the velocity is further increased (1.21 m/s $< V_p <$ 1.22 m/s), a second codimension two bifurcation occurs when two of the SN bifurcations collide and disappear, leading to a stable and an unstable branch (A). When progession velocity is further increased the third SN bifurcation reaches zero at $V_p = 1.43$ m/s (C). Furthermore, at this velocity a similar set of events take place in reverse order for long step lengths. We observe the birth of two SN bifurcations for 1.43 m/s $< V_p <$ 1.44 m/s (B). Then, one of the SN bifurcations gradually moves to the right and disappears for higher velocity values ($V_p = 1.55$ m/s).

The overall picture is depicted in Fig. (3). Solid curves in the figure represent SN bifurcations, whereas dashed curves represent crossings to negative ϕ_5^+ values. We highlighted the two regions that correspond to the events described in Fig. (2) and marked the five transition points of the figure accordingly. As Fig.(3) denotes **TYPE I** cycles are less likely to occur for shorter step lengths, faster velocities, higher clearances and smaller stance knee biases. Shortening the step length causes the biped to take a larger number of forward steps to keep up with the prescribed progression velocity, decreasing the duration of each locomotion step. This diminishes the time available to the control algorithm for restoring the prescribed motion. Increasing the progression velocity has the same effect on the duration of steps. Increasing the clearance increases the vertical velocity of the tip at contact. Higher vertical tip velocities lead to increased perturbations and may lead to the disappearance of **TYPE I** cycles.

The dashed curves that are present for low clearance values indicate that

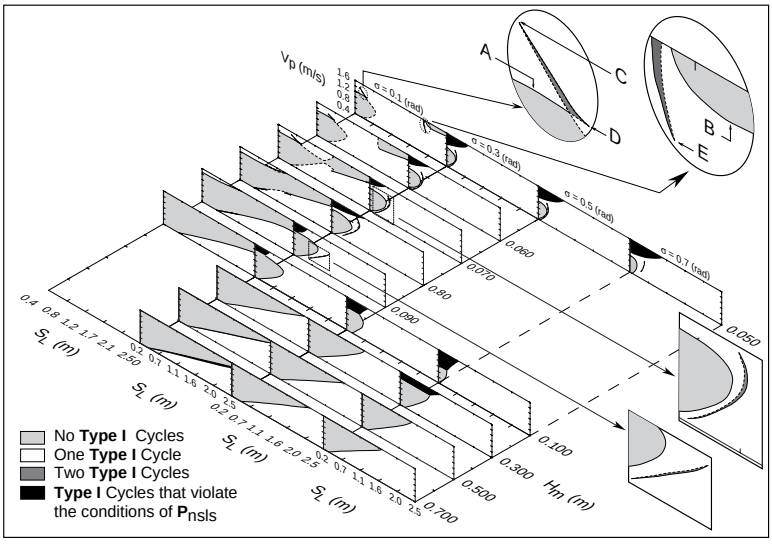

Figure 3: Bifurcation of **TYPE I** cycles.

the zero crossings occur for low clearances and short to moderate step lengths.

Zero crossings trigger a very complex pattern of bifurcations. Figure (4.a) depicts the bifurcation diagram for the parameter values shown. A variety of complex of bifurcations are apparent from the diagram. Periodic windows exist where the steady state limit cycles lock into subharmonics, there are also regions of accumulation of bifurcations.

The **TYPE II**$^{(n)}$ cycles are detected in open parameter intervals. End points of the intervals correspond to parameter values when a certain iterate of a cycle is located on the singularity plane. Therefore, the cycles cease to exist at the exact end points. Furthermore, when a particular iterate of a cycle approaches the singularity plane, a secondary cycle emerges and coexists with first cycle until the iterate moves on the singularity plane. The mapping exhibits this hysteretic behavior at every bifurcation point. Accordingly, the parameter range consists of open subintervals of **TYPE II**$^{(n)}$ cycles with overlapping portions.

The details of the first crossing is depicted in Fig. (4.b). As the **TYPE I** branch approaches the crossing point we observe the birth of a **TYPE II**$^{(10)}$ cycle at Cr1. The two cycles coexist between Cr1 and Cr2. When the eighth iterate of the period ten cycle approaches the crossing point a second period ten cycle emerges at Cr2. The former cycle disappears when its eighth iterate becomes singular at Cr3. Finally, the period one cycle disappears at Cr4.

Figure (5) depicts the phase plane picture in the Cr1-Cr2 interval. The

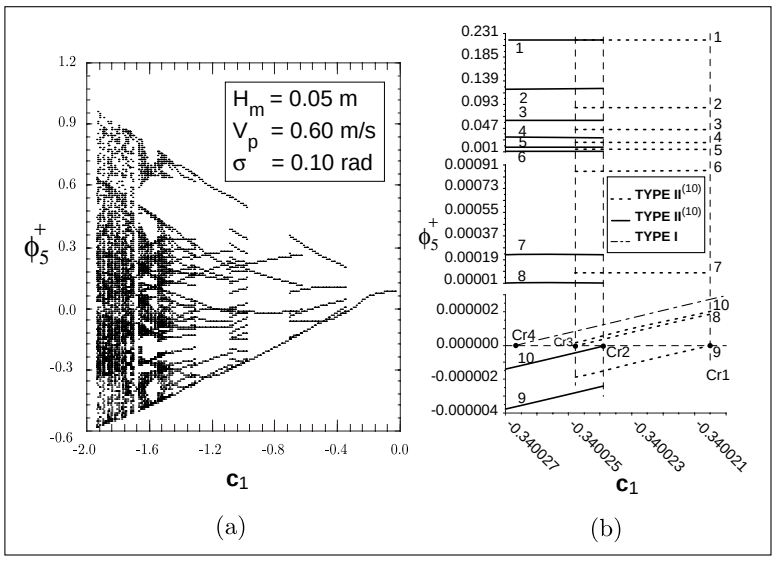

Figure 4: Zero crossing bifurcations.

darker state trajectory in the figure corresponds to the period one cycle. When a trajectory starts from an initial condition sufficiently close to the **TYPE I** cycle, it is captured by this cycle. Yet, if an initial condition is not located in the vicinity of the **TYPE I** cycle, impact and switching transfers the trajectory to the negative half plane. Following a single loop in the negative half-plane the trajectory crosses back. Then it starts to descend toward the **TYPE I** cycle. But, the trajectory crosses to the negative half plain again before it is completely captured by the period one cycle. This leads to the first period ten cycle shown if Fig. (4.b). In the parameter interval (Cr2-Cr3) three cycles coexist. A new **TYPE II**$^{(10)}$ cycle with two loops in the negative half-plane emerges. This bifurcation takes place when the destination of the loop in the negative half-plane does not cross back to the positive half-plane leading to two successive iterates in the negative half plane (see Fig. (4.b)).

The complexity of the motion for other parameter values are apparent from the bifurcation diagram. We will not elaborate on all of the aspects of the dynamic structure in this article for the sake of brevity.

5 Discussion and Conclusions

The first objective of the present article is to develop a general methodology to study the stability of bipedal locomotion without any specific assumptions

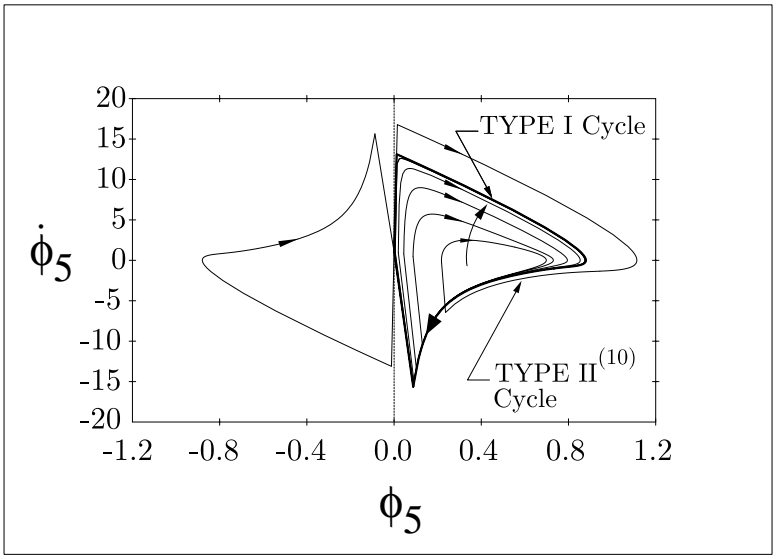

Figure 5: The Cr1 transition on the phase plane portrait.

about the internal structure of the biped. The second goal is to demonstrate the utility of the proposed methodology by using it to study the structural stability of a bipedal locomotion model with a proper parametric formulation.

We have proposed a discrete mapping technique that addresses the nonlinear and discontinuous nature of bipedal gait. The proposed approach brings a formal definition to the stability of gait and enables the utilization of the analytical tools of nonlinear dynamics to analyze the motion of a general class of bipedal locomotion systems.

The method was applied to perform study the bifurcations of a five-element bipedal locomotion model in the four-dimensional parameter space. The model was constructed by using the objective functions of Part I in conjunction with a computed torque control algorithm. The analysis demonstrated the existence of variety of gait patterns that can be radically different from the ones intended by the objective functions. The discrete mapping technique was successfully used in capturing many aspects of the motion that would have been impossible with the previous approaches that have been followed by other researchers in the bipedal locomotion area.

The bipedal model used in this study includes some idealizations such as neglecting the dynamics of the feet and assuming rigid bodies. Furthermore, the computed torque algorithm assumes perfect knowledge of system parameters and some practical issues such as the actuator dynamics and limitations of actuator torques were not considered. We believe however, the model has

successfully served to establish the main results intended by the article. More practical models equiped with realistic controllers are currently under study and will be the subject of forthcoming publications.

References

Furusho, J. and Masubichi, M., 1986, "Control of a Dynamical Biped Locomotion System for Steady Walking," *ASME Journal of Dynamic Systems, Measurement, and Control*, Vol.108, pp. 111-118.

Guckenheimer J. and Holmes P. 1985,*Nonlinear Oscillations, Dynamical Systems, and Bifurcations of Vector Fields*, Springer-Verlag, New York.

Hemami, H. and Wyman, B. F., 1979, "Modelling and Control of Constrained Dynamic Systems with Application to Biped Locomotion in the Frontal Plane," *IEEE Trans. Aut. Control*, Vol.24, pp. 526.

Hemami, H. and Chen, B. R., 1984, "Stability Analysis and Input Design of a Two-Link Planar Biped," *The International Journal of Robotics Research*, Vol.3, No.2, pp. 93-100.

Hurmuzlu, Y. and Moskowitz, G., 1987, "Bipedal Locomotion Stabilized by Impact and Switching: I. Two and Three Dimensional, Three Element Models," *Int. J Dynamics and Stability of Systems*, Vol. 2, No. 2, pp. 73-96.

Katoh, R. and Mori, M., 1984, "Control Method of Biped Locomotion Giving Asymptotic Stability of Trajectory," Automatica, Vol. 20, No. 4, pp. 405-414.

Shaw, J. and Shaw, S.W., 1989, "The Onset of Chaos in a Two-Degree-of-Freedom Impacting System," *Journal of Applied Mechanics*, Vol. 56, pp. 168-174.

Shaw S.W. and Holmes P.J., 1983, "A Periodically Forced Piecewise Linear Oscillator", *Journal of Sound and Vibration*, Vol. 90(1), pp129-155.

Vucobratovic, M., Borovac B., Surla D. and Stokic D., 1990, "*Scientific Fundamentals of Robotics 7. Biped Locomotion: Dynamics Stability, Control and Application.*" Springer-Verlag, New York.

Zheng, Y.F. 1989, "Acceleration Compensation for Biped Robots to Reject External Disturbances," *IEEE Trans. Syst. Man Cyber*, Vol. 19, No. 1, pp.74-84.

Zheng, Y.F. and Hemami, H., 1984, "Impact Effects of Biped Contact with the Environment," *IEEE Trans. Syst. Man Cyber*, Vol. SMC-14, No. 3, pp.437-443.